

Covy – An AI-powered Robot for Detection of Breaches in Social Distancing

Serge Saaybi
Delft University of Technology

Amjad Yousef Majid
Delft University of Technology

R Venkatesha Prasad
Delft University of Technology

Anis Koubaa
Prince Sultan University

Chris Verhoeven
Delft University of Technology

Abstract

We present *Covy* – a robotic platform that promotes social distancing during pandemics like COVID-19. *Covy* features a novel compound vision system that enables it to detect social distancing breaches up to 16m away. *Covy* navigates its surroundings autonomously using a hybrid navigation stack that combines Deep Reinforcement Learning (DRL) and a probabilistic localization method. We built the complete system and evaluated *Covy*'s performance through extensive sets of experiments both in simulated and realistic environments. Amongst others, our results show that the hybrid navigation stack is more robust compared to a pure DRL-based solution.

1 Introduction

The successful fight against a pandemic is partly determined by the degree to which the imposed public health measures are adhered to by the population. Enforcing these measures manually is a difficult and tiresome task if not impossible. Manual intervention in itself may lead to further spread. Technology can promote the desired social behaviors, such as social distancing and face masking without the risk of additional infections. To this end, many technological solutions have been proposed to monitor, analyze, and encourage people to follow the recommended guidelines. Examples of proposed solutions include monitoring through closed-circuit television (CCTV) [27] or tracking via cellular networks, wearables and smartphones [24]. While the former has no straightforward way of providing feedback to people, the latter compromise their privacy.

We look towards autonomous Robots that can support humans in this situation. They are mobile and can relatively easily be equipped with means to interact with humans and encourage desired social behaviors (e.g. alerting littering individuals). Nonetheless, a single robot, no matter how advanced, (e.g., Spot from Boston Dynamics [12]) would not provide adequate coverage as it can only cover limited areas. A better alternative is to employ a swarm of collaborating robots.

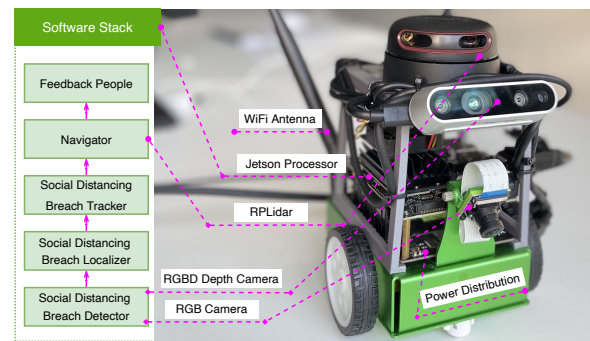


Figure 1: Hardware and software overview of *Covy*: a prototype swarm robot for promoting social distancing practice.

However, to make the swarm solution viable, the cost of manufacturing the robots should be kept to a minimum while meeting the application requirements. Towards this end, we developed *Covy* – a low-cost robot that has a unique vision system and a hybrid navigation stack.

Challenges. While there are many aspects to building a robot for such a purpose, we provide herewith only relevant challenges. *Covy* was developed with two main challenges in mind: ❶ Designing a long-range, low-cost vision system that can estimate the 3D coordinates of people in the scene; and ❷ Developing a navigation stack that is generalizable and easily deployable on different robot models.

Contributions. Our contributions are manifold. ❶ We built a platform with complete stack called *Covy* and used it for evaluation. ❷ We developed a *compound algorithm* that increases the effective range of the Intel RealSense depth camera by two times for detecting social distancing breaches. ❸ We developed a hybrid navigation stack that combines the power of Deep Reinforcement Learning and a probabilistic localization system. ❹ We evaluated *Covy* by conducting extensive experiments in simulated and realistic environments.

2 Related work

The use of robots for surveillance has been suggested before. Dr. spot is a teleoperated quadruped robot that monitors social distancing and face masking in public space and alerts offenders [30]. Chen et al. [6] introduced a fully autonomous yet expensive surveillance quadruped, meaning large-scale production for encouraging desired social behavior will be costly. Therefore, Sathyamoorthy et al. [28] proposed a low-cost robotic system – similar to Covy – able to detect and navigate towards the breaches using an RGB-D camera and 2D lidar. Their system also leverages static CCTV to increase the detection range. However, a major drawback is the limited detection range of only up to 4 m for the mounted depth camera and 3 m for the fixed CCTV. We, in this work, propose a compound low-cost vision system with a breach detection range of up to 16+ m.

There is a growing interest in robotic navigation based on different DRL algorithms [14, 22, 31, 32]. This is driven mainly by the portability of a DRL navigation stack onto different robotic platforms and the capability for online learning. Tai et al. [32] used Deep Deterministic Policy Gradient (DDPG) to develop a mapless motion planner able to navigate a robot in real unseen environments with obstacles. Costa de Jesus et al. [7] replaced the DDPG with the Soft Actor-Critic [9] (SAC) DRL model and showed its efficacy through simulation. Long et al. [20] utilized Proximal Policy Optimization (PPO) [29] for a multi-robot collision avoidance policy directly mapping raw sensor measurements to an agent’s steering commands. They also validated the policy in various simulated environments. Kulhánek et al. [17] developed a purely camera-based navigation system by extending a version of the batched A2C algorithm [22] and validated the performance on a real robot [18]. For Covy, we experimented with DDPG and SAC, a deterministic and probabilistic DRL model, and developed a hybrid navigation stack to overcome some of the observed limitations in a pure DRL approach.

3 Systems Overview

3.1 Hardware

Figure 1 shows Covy’s hardware and software stack. We explain briefly the Covy system below.

Main CPU. Covy is based on the Jetson single-board computer family that is capable of running multiple neural networks on low power. Jetson processor family includes Jetson Nano, Jetson Xavier NX, and Jetson Xavier AGX.

Vision Sensor. An RGB-D camera captures RGB images and their depth information on a per-pixel basis [21]. As such it is the natural choice for estimating 3D coordinates of objects in images. The two most suitable depth cameras for our applications are the ZED2 [3] and the Intel RealSense D435i [23]. The ZED2 has twice the depth range of the D435i but also costs twice as much. We chose to work with the lower-

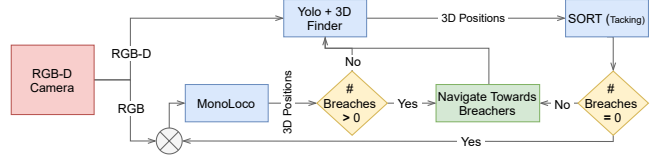


Figure 2: Schematic of the compound vision system of Covy.

cost D435i which has a nominal depth range of 10 m.

Robot body. As we target indoor environment we equipped Jetbot [1] with a 2D lidar [2] to enable the robot to navigate autonomously within a building.

3.2 Software

Covy has a ROS-based [25] software that is divided into two main modules: breach detection and navigation.

3.2.1 Breach Detection

Covy vision system scans the scene for people twice: (i) Using RGB-D images, Covy localizes nearby people, and (ii) using pure RGB images, it estimates the localization of people that cannot be detected in the first stage (Figure 2). In stage one, YOLOv3 ROS [26] takes in an RGB image and identifies the people in it. Then, it publishes three ROS topics: bounding boxes around identified objects, their categories, and confidence scores. To determine the 3D coordinates of identified people, Covy obtains the depth information from the RealSense depth camera and lays over the images published by YOLOv3. The obtained 3D coordinates are then sent to the SORT [5] algorithm to track people across multiple images.

SORT utilizes both the position and size of the bounding box for motion estimation and data association using the Kalman filter and Hungarian method respectively and outputs unique IDs for each identified pedestrian. After tracking the identified pedestrians for 20 frames, their 3D coordinates are averaged and the inter-person distance is calculated using the Euclidean distance measure. If the distance between two individuals is less than the specified threshold (e.g., 1.5 m Covy reports a breach. This process is repeated pairwise for all the detected individuals. The result is a list of breaches containing the different groups of non-compliant pedestrians. Covy determines the largest group, computes its middle coordinates and sends these to the navigation module (Figure 2). Since depth information is only available at a short-range (our experiments show an effective range of 6 m), when no individuals are detected Covy switches to MonoLoco [4] for long-range scanning (i.e., up to 20 m). MonoLoco processes RGB images as a set of 2D joints using two pose detectors: Mask R-CNN [11], which works top-down, and OpenPifPaf [16], which works bottom-up. Then, the MonoLoco [4] algorithm takes these 2D joints as input and outputs the 3D locations, orientations, and dimensions of the detected people together

with localization uncertainty. Finally, the system publishes an approximation of each pedestrian’s x , y , z coordinates identified in the image along with their status and any corresponding breaches. The navigation module then guides Covy towards the largest breach density. Using this compound procedure Covy triple the effective range of Intel RealSense at no additional costs.

3.2.2 Navigation

We have experimented with two different DRL algorithms to navigate Covy in different environments. Deep Deterministic Policy Gradient (DDPG, Figure 3a) and Soft Actor-Critic (SAC, Figure 3b). These agents have actor-critic network architectures that act in continuous action space [19] (Figure 3). The environment is observed through 10 laser range findings emitted in a range from -90° to 90° , 0° being the middle front of the robot. These laser scans are concatenated with the angular and linear velocity and with the position and heading angle of the robot relative to the target to form the input state of the DRL agents (Figure 3, $\text{input}(s_t) | 14$). The position and heading of the robot are determined using the rf2o [13] Lidar odometry approach which relies purely on Lidar scan measurements to determine the robots change in position. In DDPG, a \tanh activation function is applied to the angular velocity output layer to limit the range to $[-2, 2]$, and a sigmoid activation function is applied to the linear velocity output layer to limit the range to $[0, 0.2]$. As for SAC, it uses the \tanh activation function and the clip operation to similarly limit its linear and angular velocities. Since the laser readings only record data in front of the robot only positive linear velocity is considered (i.e., no backward motion is allowed or considered). Our DDPG network configuration is based on [7, 32] with minor modifications to the critic. As for SAC, we used the network from [33], and omitted the value network, as mentioned in [10]. To train the DRL agents the following reward function is:

$$r(s_t, a_t) = \begin{cases} r_a & \text{if } D_t < T \\ r_c & \text{if } \min_c < L_t \\ r_{d1}(D_{t-1} - D_t) & \text{if } (D_{t-1} - D_t) > 0 \\ r_{d2} & \text{if } (D_{t-1} - D_t) \leq 0 \end{cases}$$

There are four different conditions for the reward system. If the robot reaches the goal within a predefined time threshold T , it receives a big positive reward. If the lidar reading L_t is smaller than the minimum allowed \min_c then a negative reward is given as the robot is about to collide or has collided. Compared to the previous position, if the current robot position is closer to the target, the robot gets a positive reward proportional to its advancements. Otherwise, it is penalized. **Hybrid Autonomous Navigation.** When testing the DRL navigation agents, we noticed that the error in the Lidar odometry can become suddenly too large causing the robot to lose track. Whenever this happens the navigation fails and the robot is unable to reach its target.

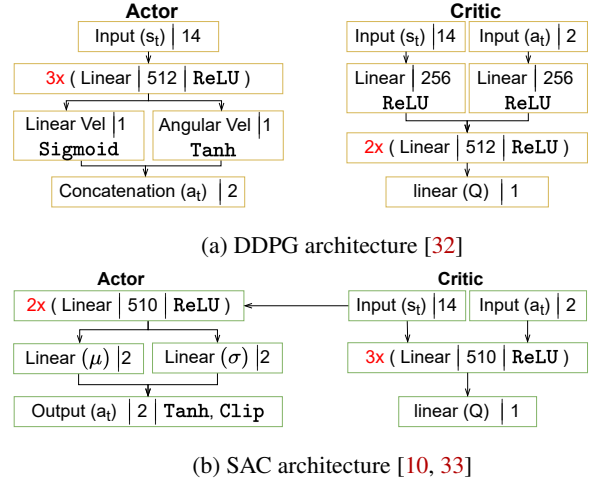


Figure 3: DRL models used for navigation

To counter this unwanted behavior, we developed a hybrid navigation stack that combines the DRL mapless navigation with a map-based localization algorithm, namely, the Adaptive Monte Carlo Localization (AMCL) [8] method. First, the SAC DRL agent navigates the robot towards a target using Lidar odometry. Then, for every X step (in our case, $X = 20$) Covy compares the Lidar odometry output to the pose estimation obtained from AMCL. If the difference between the two positions is higher than a preset threshold, Covy reinitializes its position and orientation based on the output of the AMCL algorithm.

4 Experimental Evaluation

4.1 Vision System

Two sets of experiments were conducted to evaluate Covy’s vision system – person’s location estimation accuracy and classification accuracy of breaches in social distancing. For the former, a person moves away from the camera by 1 m, and for the latter, two pedestrians stood at various coordinates in the scene. We ensured that the people were in the field of view of the camera and took 50 pictures at each location. For the classification experiments, balanced data was ensured. These experiments were conducted in a simulated and real environment and repeated until the camera could not detect any pedestrian. Finally, we profiled the execution of these algorithms on Jetson Nano and Jetson Xavier NX.

4.1.1 Localization

Figure 4 shows the average localization error (ALE) of Covy’s vision RGB-D and RGB localization methods. We can observe that the RGB-based method has a range 2.4 x and 4.3 x longer than RGB-D in the real and simulated environment, respectively. However, for proximity scanning, the RGB-D method has a higher localization accuracy. Therefore, by com-

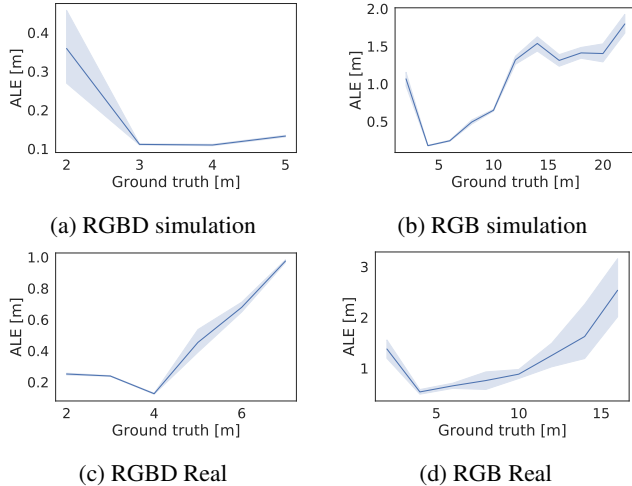


Figure 4: Average localization error (ALE) with confidence interval as a function of distance – RGBD and RGB based system.

Method	Accuracy (%)	Precision (%)	Recall (%)	Env.
RGB-D	96	98	95	Sim.
RGB	92	96	88	Sim.
RGB-D	82	90	72	Real
RGB	82	93	70	Real

Table 1: Accuracy of classifying social distancing breaches

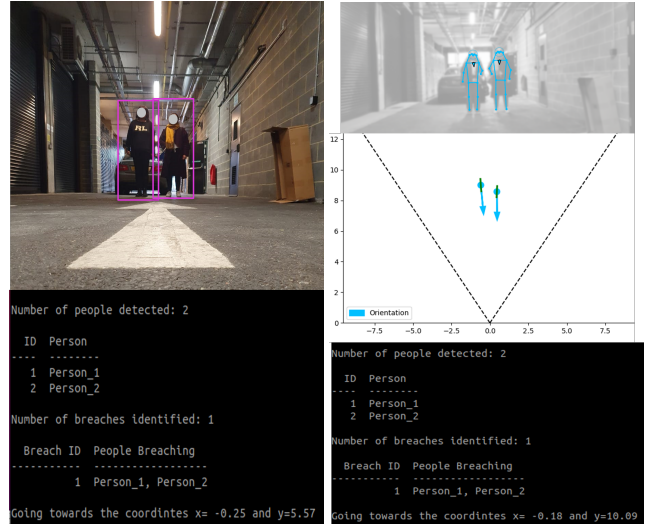
binning these two coating methods Covy can localize people at a long-range and with increased accuracy.

4.1.2 Accuracy of Classification of Breaches

This experiment compares the performance of the RGB-D and RGB-based vision systems in detecting social distancing violations. We treat the problem as a binary classification task and evaluate the detection accuracy, recall, and precision. Figure 6 shows the confusion matrices for the RGB-D and RGB breach detection, and Table 1 compares the accuracy, precision, and recall between them. First, we notice a drop in the performance of both methods when moving from simulated to the real world. This is mainly due to the increase in the ALE (as shown in Figure 4). However, while the RGB-D method performs better in simulation, the margin in performance between the two methods shrinks in reality. This is due to the ratio at which the ALE changes in the simulated and real environment of both methods. Overall, both algorithms maintained an accuracy equal to 82%. Qualitative results of both methods are shown in Figure 5. Combined, these results show the promising ability of these approaches in recognizing breaches in social distancing.

4.1.3 Hardware Requirements

After testing the accuracy of the two breach detection systems, we deployed them on the intended edge devices to profile their



(a) RGBD qualitative results (b) RGB qualitative results

Figure 5: Example of Covy’s vision modules (i.e., RGB and RGB-D) and detection accuracy of breaches.

Table 2: Performance comparison of breach detection algorithms on different hardware.

Processor	Algorithm	CPU (%)	GPU (%)	Memory (GB)
Nano	Idle	15	3	1.6/4.1
	RGB-D	99	83	2.7/4.1
	RGB	NA	NA	NA
Xavier NX	Idle	14	1	2.5/8
	RGB-D	58	15	3.3/8
	RGB	39	59	7.2/8
	Covy’s vision	70	63	7.4/8

execution. We tested the performance in terms of CPU, GPU, and memory usage. Firstly, we measured the resources utilization levels at an idle condition. Then, we let the model reach its steady-state behavior by running it for a few minutes. Finally, 100 performance measurements were taken and averaged out (Table 2).

Jetson Nano was able to run the RGB-D detection system based on Yolov3 [26], but reached maximum CPU utilization ($\approx 99\%$) and very high GPU utilization (83%). Moreover, Jetson Nano was unable to run the resource-intensive RGB-based detection algorithm which runs multiple DL models to estimate the 3D coordinates of people in the scene.

Jetson Xavier NX was able to run both systems adequately keeping peak GPU utilization (59%) and peak CPU utilization (58%) at acceptable levels. However, the RGB system consumed most of the available memory averaging 7.2 GB RAM usage out of the total 8.

Considering that the individual performances were favorable, we tested Covy’s vision algorithm as a whole on Jetson

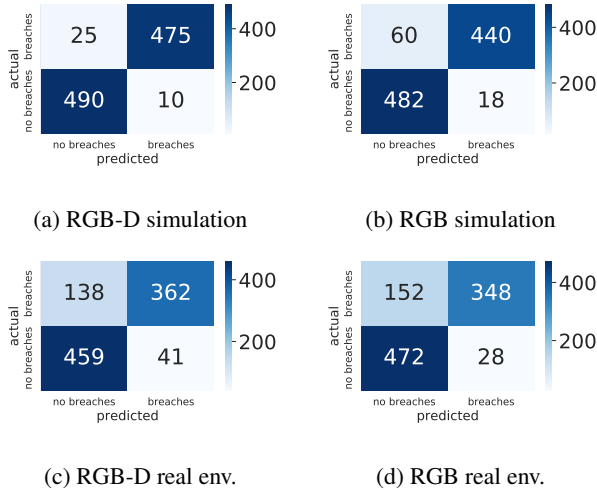


Figure 6: Accuracy in Detection of Breaches Using Covy’s Vision Modules (RGB and RGB-D) in simulated and real environment.

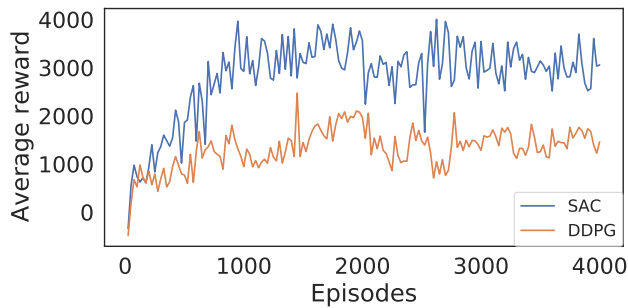


Figure 7: Training in environment with static and dynamic obstacles.

Xavier NX. The overall performance seemed promising, with the highest average utilization reaching 70% for CPU, 63% for GPU utilization, and 7.4 GB for RAM usage.

4.2 Navigation

Covy’s navigation is evaluated using three metrics: the time to goal, the distance to the goal and the failure rate which includes collisions and deadlocks.

4.2.1 DRL Agents Training

We trained the DDPG and SAC models on a computer equipped with an NVIDIA GeForce GTX 1060, 16 GB of RAM, and an Intel Core i7-8750H processor. The models were trained for 4000 episodes on a Jetbot robot model in a $4 \times 4 \text{ m}^2$ room-like simulated environment with either: no obstacles, static obstacles, or dynamic obstacles [15]. After training completion, we tested the models’ capabilities in a simulated and real environment by sampling 35 random configurations from the aforementioned environments.

Table 3: DDPG vs SAC. Results averaged over 100 episodes.

DRL	Failure (%) (collision/lost)	Average Speed (m/s)	Env.
DDPG	13 (8 / 5)	0.125	Sim.
DDPG	26 (15 / 11)	0.099	Real
SAC	8 (6 / 2)	0.17	Sim.
SAC	20 (8 / 12)	0.13	Real
Hybrid	7 (7 / 0)	0.046	Sim.
Hybrid	10 (10 / 0)	0.057	Real

Figure 7 shows the cumulative rewards obtained by DDPG and SAC during training in an environment with static and dynamic obstacles where each data point represents the average reward over 25 episodes. After ≈ 350 episodes, SAC surpasses DDPG in performance constantly. SAC reached a maximum average reward of approximately 3000, double that of DDPG. We hypothesize that as SAC is a stochastic policy, it is able to explore better the environment and therefore collect higher rewards.

4.2.2 Navigation Accuracy

From Table 3 we see that the SAC model performs better than the DDPG model in terms of the failure rate. Additionally, SAC is faster than DDPG in reaching the target: we suspect that the stochastic nature of SAC provides better exploration and allows the model to find an optimal path, whereas DDPG is deterministic. An interesting observation is that both DDPG and SAC can get lost (or end up in a deadlock) in simulated and real environments. We conjecture that this is due to the use of Lidar odometry which can produce inconsistent measurement when the robot moves fast. However, our hybrid approach is designed to overcome this limitation and performs best with respect to the failure rate at the cost of slower navigation.

5 Conclusion and Future Work

Covy is a prototype designed to test a compound vision system and different navigation stacks. The target application is to promote social distancing practice during a pandemic (e.g., COVID-19). The compound algorithm that Covy uses extends the range of depth of the Intel RealSense D435i camera from an effective range of 6m to 16+ m. Covy navigates its surroundings autonomously using a hybrid navigation stack that combines a SAC (DRL) agent with the probabilistic localization method AMCL. compared to a pure DRL-based navigation stack, Covy’s stack performs better in navigating in realistic and simulated environments with static and dynamic obstacles. Next step is to develop a complete swarm of Covy robots and target other applications such as alerting littering individuals, finding objects of interest, e.g., security of airports.

References

- [1] Jetbot: An AI driven robot. URL <https://www.waveshare.com/jetbot-ai-kit.htm>.
- [2] Rplidar A2: a laser range scanner. URL <https://www.slamtec.com/en/Lidar/A2>.
- [3] Zed 2: An AI stereo camera. URL <https://www.stereolabs.com/zed-2i/>.
- [4] Lorenzo Bertoni, Sven Kreiss, and Alexandre Alahi. Monoloco: Monocular 3d pedestrian localization and uncertainty estimation. In *Proceedings of the IEEE/CVF International Conference on Computer Vision*, pages 6861–6871, 2019.
- [5] Alex Bewley, Zongyuan Ge, Lionel Ott, Fabio Ramos, and Ben Uptcroft. Simple online and realtime tracking. *2016 IEEE International Conference on Image Processing (ICIP)*, Sep 2016. doi: 10.1109/icip.2016.7533003. URL <http://dx.doi.org/10.1109/ICIP.2016.7533003>.
- [6] Zhiming Chen, Tingxiang Fan, Xuan Zhao, Jing Liang, Cong Shen, Hua Chen, Dinesh Manocha, Jia Pan, and Wei Zhang. Autonomous social distancing in urban environments using a quadruped robot. *IEEE Access*, 9: 8392–8403, 2021.
- [7] Junior Costa de Jesus, Victor Kich, Alisson Kolling, Ricardo Grando, Marco Cuadros, and Daniel Fernando Gamarra. Soft actor-critic for navigation of mobile robots. *Journal of Intelligent & Robotic Systems*, 102, 06 2021. doi: 10.1007/s10846-021-01367-5.
- [8] Dieter Fox, Wolfram Burgard, Frank Dellaert, and Sebastian Thrun. Monte carlo localization: Efficient position estimation for mobile robots. *AAAI/IAAI*, 1999 (343-349):2–2, 1999.
- [9] Tuomas Haarnoja, Aurick Zhou, Pieter Abbeel, and Sergey Levine. Soft actor-critic: Off-policy maximum entropy deep reinforcement learning with a stochastic actor. In *International conference on machine learning*, pages 1861–1870. PMLR, 2018.
- [10] Tuomas Haarnoja, Aurick Zhou, Kristian Hartikainen, George Tucker, Sehoon Ha, Jie Tan, Vikash Kumar, Henry Zhu, Abhishek Gupta, Pieter Abbeel, et al. Soft actor-critic algorithms and applications. *arXiv preprint arXiv:1812.05905*, 2018.
- [11] Kaiming He, Georgia Gkioxari, Piotr Dollár, and Ross Girshick. Mask r-cnn. In *Proceedings of the IEEE international conference on computer vision*, pages 2961–2969, 2017.
- [12] Hen-Wei Huang, peter chai, Claas Ehmke, Gene Merewether, Fara Dadabhoy, Annie Feng, Akhil John Thomas, Canchen Li, Marco da Silva, Marc H Raibert, et al. Agile mobile robotic platform for contactless vital signs monitoring. 2020.
- [13] Mariano Jaimez, Javier G. Monroy, and Javier Gonzalez-Jimenez. Planar odometry from a radial laser scanner: a range flow-based approach. In *2016 IEEE International Conference on Robotics and Automation (ICRA)*, pages 4479–4485, 2016. doi: 10.1109/ICRA.2016.7487647.
- [14] Gregory Kahn, Adam Villaflor, Bosen Ding, Pieter Abbeel, and Sergey Levine. Self-supervised deep reinforcement learning with generalized computation graphs for robot navigation. In *2018 IEEE International Conference on Robotics and Automation (ICRA)*, pages 5129–5136. IEEE, 2018.
- [15] Nathan Koenig and Andrew Howard. Design and use paradigms for gazebo, an open-source multi-robot simulator. In *2004 IEEE/RSJ International Conference on Intelligent Robots and Systems (IROS)(IEEE Cat. No. 04CH37566)*, volume 3, pages 2149–2154. IEEE, 2004.
- [16] Sven Kreiss, Lorenzo Bertoni, and Alexandre Alahi. Pif-paf: Composite fields for human pose estimation. In *Proceedings of the IEEE/CVF conference on computer vision and pattern recognition*, pages 11977–11986, 2019.
- [17] Jonáš Kulhánek, Erik Derner, Tim De Bruin, and Robert Babuška. Vision-based navigation using deep reinforcement learning. In *2019 European Conference on Mobile Robots (ECMR)*, pages 1–8. IEEE, 2019.
- [18] Jonáš Kulhánek, Erik Derner, and Robert Babuška. Visual navigation in real-world indoor environments using end-to-end deep reinforcement learning. *IEEE Robotics and Automation Letters*, 6(3):4345–4352, 2021.
- [19] Timothy P Lillicrap, Jonathan J Hunt, Alexander Pritzel, Nicolas Heess, Tom Erez, Yuval Tassa, David Silver, and Daan Wierstra. Continuous control with deep reinforcement learning. *arXiv preprint arXiv:1509.02971*, 2015.
- [20] Pinxin Long, Tingxiang Fan, Xinyi Liao, Wenxi Liu, Hao Zhang, and Jia Pan. Towards optimally decentralized multi-robot collision avoidance via deep reinforcement learning. In *2018 IEEE International Conference on Robotics and Automation (ICRA)*, pages 6252–6259. IEEE, 2018.
- [21] Zhihan Lv, Jaime Lloret Mauri, and Houbing Song. Editorial rgb-d sensors and 3d reconstruction. *IEEE Sensors Journal*, 20(20):11751–11752, 2020.

- [22] Amjad Yousef Majid, Serge Saaybi, Tomas van Rietbergen, Vincent Francois-Lavet, R Venkatesha Prasad, and Chris Verhoeven. Deep reinforcement learning versus evolution strategies: A comparative survey. *arXiv preprint arXiv:2110.01411*, 2021.
- [23] Chiranjivi Neupane, Anand Koirala, Zhenglin Wang, and Kerry Brian Walsh. Evaluation of depth cameras for use in fruit localization and sizing: Finding a successor to kinect v2. *Agronomy*, 11(9):1780, 2021.
- [24] Cong T. Nguyen, Yuris Mulya Saputra, Nguyen Van Huynh, Ngoc-Tan Nguyen, Tran Viet Khoa, Bui Minh Tuan, Diep N. Nguyen, Dinh Thai Hoang, Thang X. Vu, Eryk Dutkiewicz, and et al. A comprehensive survey of enabling and emerging technologies for social distancing—part i: Fundamentals and enabling technologies. *IEEE Access*, 8:153479–153507, 2020. ISSN 2169-3536. doi: 10.1109/access.2020.3018140. URL <http://dx.doi.org/10.1109/ACCESS.2020.3018140>.
- [25] Morgan Quigley, Ken Conley, Brian Gerkey, Josh Faust, Tully Foote, Jeremy Leibs, Rob Wheeler, and Andrew Ng. Ros: an open-source robot operating system. volume 3, 01 2009.
- [26] Joseph Redmon and Ali Farhadi. Yolov3: An incremental improvement. *arXiv preprint arXiv:1804.02767*, 2018.
- [27] Mahdi Rezaei and Mohsen Azarmi. Deepsocial: Social distancing monitoring and infection risk assessment in covid-19 pandemic. *Applied Sciences*, 10(21):7514, Oct 2020. ISSN 2076-3417. doi: 10.3390/app10217514. URL <http://dx.doi.org/10.3390/app10217514>.
- [28] Adarsh Jagan Sathyamoorthy, Utsav Patel, Yash Ajay Savle, Moumita Paul, and Dinesh Manocha. Covid-robot: Monitoring social distancing constraints in crowded scenarios. *CoRR*, 2020.
- [29] John Schulman, Filip Wolski, Prafulla Dhariwal, Alec Radford, and Oleg Klimov. Proximal policy optimization algorithms. *arXiv preprint arXiv:1707.06347*, 2017.
- [30] Yang Shen, Dejun Guo, Fei Long, Luis A Mateos, Houzhu Ding, Zhen Xiu, Randall B Hellman, Adam King, Shixun Chen, Chengkun Zhang, et al. Robots under covid-19 pandemic: A comprehensive survey. *Ieee Access*, 2020.
- [31] Hartmut Surmann, Christian Jestel, Robin Marchel, Franziska Musberg, Housseem Elhadj, and Mahbube Ardani. Deep reinforcement learning for real autonomous mobile robot navigation in indoor environments. *arXiv preprint arXiv:2005.13857*, 2020.
- [32] Lei Tai, Giuseppe Paolo, and Ming Liu. Virtual-to-real deep reinforcement learning: Continuous control of mobile robots for mapless navigation. In *2017 IEEE/RSJ International Conference on Intelligent Robots and Systems (IROS)*, pages 31–36. IEEE, 2017.
- [33] Jiaqi Xiang, Qingdong Li, Xiwang Dong, and Zhang Ren. Continuous control with deep reinforcement learning for mobile robot navigation. In *2019 Chinese Automation Congress (CAC)*, pages 1501–1506. IEEE, 2019.